Süleyman Demirel Üniversitesi
Fen Bilimleri Enstitüsü Dergisi
Cilt 30, Sayı 1, 106-113, 2026

Süleyman Demirel University
Journal of Natural and Applied Sciences
Volume 30, Issue 1, 106-113, 2026

DOI: 10.19113/sdufenbed.1789977

Effect of Magnet Spacing on Magnetic Field Linearity in Selected Commercial Rectangular Magnets

Samed GÜMÜŞ*[1], Yavuz ÖZTÜRK[2]

[1]Izmir Institute of Technology, Faculty of Science, Physics, 35433, Izmir, Türkiye

[2]Ege University, Faculty of Engineering, Electrical and Electronics Engineering, 35040, Izmir, Türkiye

(Alınış / Received: 23.09.2025, Kabul / Accepted: 21.01.2026, Online Yayınlanma / Published Online: 24.04.2026)

Keywords
Bar magnet,
Magnetic levitation,
Magnetic field linearity.

Abstract: In density measurements using magnetic levitation and in magnetic sensor applications, the linearity of the magnetic field and magnetic force is important for measurement convenience. In line with this purpose, an analysis was conducted on a sample magnet configuration with dimensions of 3×60×10 mm to show influence of magnet spacing on the magnetic field linearity. Additionally, the most commonly used magnet dimensions in industry were selected, and the analyses were repeated for each set individually. For each configuration, the distance between the magnets varied between 1 mm and 10 mm, and for each distance, the magnetic field distribution along the magnetization direction on the central axis of the magnets was calculated and fitted to a linear function. Linearity in these fitting processes was evaluated using the R^2 and RMSE metrics. The highest value of R^2 = 0.9999 and lowest value of RMSE=0.25 mT was obtained for the magnet spacing of 2 mm.

Mıknatıs Aralığının Manyetik Alan Doğrusallığına Etkisinin Ticari Dikdörtgen Mıknatıslarda İncelenmesi

Anahtar Kelimeler
Çubuk mıknatıs,
Manyetik levitasyon,
Manyetik alan doğrusallığı.

Öz: Manyetik levitasyon kullanılarak yapılan yoğunluk ölçümlerinde ve manyetik sensör uygulamalarında, manyetik alanın ve manyetik kuvvetin doğrusallığı ölçüm kolaylığı açısından önemlidir. Bu amaca uygun olarak, manyetik alan doğrusallığı üzerindeki mıknatıslar arası mesafenin etkisini göstermek için 3×60×10 mm boyutlarında örnek bir mıknatıs konfigürasyonu üzerinde bir analiz yapılmıştır. Ek olarak endüstride sıklıkla kullanılan ticari mıknatıs boyutları seçilerek aynı analizler tekrarlanmıştır. Her bir konfigürasyon için, mıknatıslar arasındaki mesafe 1 mm ile 10 mm arasında değiştirilmiş ve her mesafe için, mıknatısların merkez ekseni boyunca manyetizasyon yönündeki manyetik alan dağılımı hesaplanmış ve doğrusal bir fonksiyona uydurulmuştur. Bu uydurma süreçlerindeki doğrusallık, R^2 ve RMSE metrikleri kullanılarak değerlendirilmiştir. R^2 = 0.9999 en yüksek değeri ve RMSE = 0.25 mT en düşük değeri 2 mm'lik mıknatıs aralığı için elde edilmiştir.

1. Introduction

Magnetic systems constructed with magnet pairs same poles facing each other (Anti-Helmholtz configuration) are frequently used in several biomedical and sensor applications such as magnetic levitation, cell separation systems, flow focusing, and density measurement [1-5].

It can be summarized the example applications as follows. It has been shown that magnetic levitation systems can be used to observe cell developments or for disease diagnosis [6]. Magnetic levitation systems, which are based on the principle of suspending objects using magnetic fields, offer high sensitivity compared to traditional density measurement methods. This emphasizes the importance of designing magnet systems with same poles facing each other [7]. This configuration of magnets can also be exploited to enhance the sensitivity and consistency of displacement sensors developed using Hall sensors [8, 9]. In the literature, linear magnetic sensors employed as alternatives to standard displacement sensors for small-angle and displacement measurements provide excellent sensitivity while offering greater robustness against external influences such as dust, dirt, and

*Corresponding author: samedgms@outlook.com

temperature variations compared to interferometry-based sensors [10]. Moreover, because the magnetic moments of electrons can interact with magnets, it is possible to create magnetic atom traps at low temperatures [11]. Under appropriate conditions, systems with magnets facing each other with same poles can generate an almost linear magnetic field in the region between them, along the magnetization direction. A linear magnetic field offers several advantages for physical applications. The product of the magnetic field and its gradient yields a term related to force. The near linearity of this term simplifies the calculation of forces. Furthermore, the ease of detecting small variations in a nearly linear magnetic field positively contributes to the sensitivity of sensor applications [8]. Despite their widespread use, analytical studies on magnet pairs in this configuration are limited. In other studies, utilizing nearly linear magnetic fields, a single type of configuration designed with commercial computer simulation tools are commonly employed [1, 12]. However, these simulation tools are, not always readily accessible. Therefore, in order to employ commercially available magnet pairs in applications such as magnetic levitation, the magnetic field—as a function of the gap between the magnets—can be analytically investigated. Magnetic systems in this configuration can be constructed using permanent magnets of various geometries, such as cylindrical, rectangular prism, and ring-shaped magnets. The magnetic fields generated by such magnets can be analytically calculated [13, 14]. For a selected magnet geometry, nearly linear regions can be formed between the magnets by finding optimum gap between them. In addition, many studies in the literature have employed custom-made magnet pairs [1], which limits their accessibility. Therefore, the use of commercially available magnets is essential for low-cost applications, particularly in biomedical fields.

In this study, the magnetic field generated between an example rectangular magnet pair with same poles facing each other was analytically calculated for different gaps along the magnetization direction. Selected commercially available magnet pairs were investigated with consideration of their dimensions. The computed magnetic fields were fitted to linear functions. The agreement between the magnetic field and the linear function was evaluated using R^2 and RMSE metrics. Based on these analyses, the optimal air gap for the selected magnet geometry was determined.

2. Theoretical Method

A single magnet and a pair of magnets in anti-Helmotz geometry is shown in Figure 1. The distance between the magnets is denoted as "g", while the magnet's length, thickness, and height are represented as "2a", "2b", and "2c", respectively. The center of the air gap between the magnets is defined as z=0. When the magnetic field of a single magnet is considered, and the magnet center is set at z=0, the magnetic field in the z-direction along the z-axis (at x=0, y=0) is given as $Bs_z(z)$.

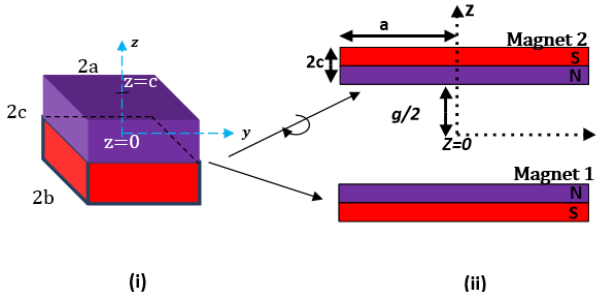

Figure 1. (i) A rectangular magnet and (ii) the pair of magnets with the same poles facing each other.

The magnetic field of single magnet in Figure 1.i can be calculated using the magnetic charge density approach. In this approach, the surface charge density is given by $\sigma = \vec{M}\hat{n}$ where M represents the magnetization. For a material with uniform magnetization ($\vec{M} = M\hat{z}$), the surface charge density at $z = c$ is $\sigma = M$, while at $z = -c$, it is $-\sigma$. Using this approach, the magnetic field of a single magnet in the z direction at any point $O(x, y, z)$ in space is given in Equation 1.

$$Bs_z = \int_{-b}^{b}\int_{-a}^{a}\left(\frac{\mu_0\sigma_s(z+c)}{4\pi[(x-x')^2+(y-y')^2+(z+c)^2]^{3/2}} - \frac{\mu_0\sigma_s(z-c)}{4\pi[(x-x')^2+(y-y')^2+(z-c)^2]^{3/2}}\right)dx'dy' \quad (1)$$

If an analytical solution is performed for points located on the symmetry axis of the magnet $O(0,0,z)$ as shown in Figure 1, the magnetic field function of the single magnet can be expressed as given in Equation 2.

$$Bs_z(0,0,z) = \frac{\mu_0 M}{\pi}\left[\arctan\left(\frac{ab}{(z-c)\sqrt{a^2+b^2+(z-c)^2}}\right) - \arctan\left(\frac{ab}{(z+c)\sqrt{a^2+b^2+(z+c)^2}}\right)\right] \quad (2)$$

In Equations (1) and (2), $\mu_0$denotes the permeability of free space. In this study, the magnetization values for analytical calculations were determined based on the residual flux density (B_r) ranges provided in commercial datasheets for N35 and N52 grade magnets (e.g., K&J Magnetics, Jinmagnets). For these grades Br typically ranges from 1.17 T to 1.48 T, which corresponds to magnetization values between approximately 931 kA/m and 1178 kA/m, according to the relation M = Br/ $M = B_r/\mu_0$. Consequently, magnetization values of 930 kA/m for N35 and 1200 kA/m for N52 were adopted for the calculations. Given

that M and Br values vary between batches and manufacturers, it is strongly recommended to measure the actual Br values and calculate the precise magnetization before utilizing magnets in high-accuracy sensor applications.

$Bs_z(0,0,z)$ in Equation (2), was calculated for selected magnet dimensions in the region z > c, and its variation along the z-axis is shown in Figure 2. Figure 2 illustrates the nonlinear variation of the magnetic field along the z-axis. The nonlinear dependence poses challenges for calculations in various sensor applications. Hence, a more linear magnetic field is required, particularly for applications involving magnetic levitation and displacement sensing.

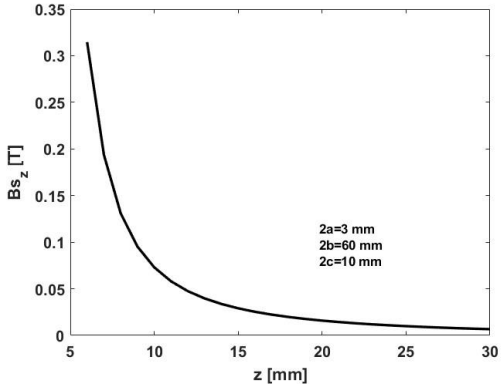

Figure 2. The graph of $Bs_z(0,0,z)$ in the region c<z (M=920 kA/m, 2a=3 mm, 2b=60 mm, 2c=10 mm).

The magnetic field equations for the magnets shifted by ±Δ (Δ= $c + g/2$) along the center z-axis are given as $B_{1z}(z)$ and $B_{2z}(z)$. These equations are expanded into a Taylor series around z=0, yielding Equation 3 and Equation 4.

$$B_{1z}(z) = Bs_z(z-\Delta) = a_0 - a_1 z + a_2 z^2 - a_3 z^3 + \cdots \quad (3)$$

$$B_{2z}(z) = -Bs_z(z+\Delta) = -a_0 + a_1 z - a_2 z^2 + a_3 z^3 + \cdots \quad (4)$$

In this case the total magnetic field is given by equation 3.

$$B_z(z) = B_{1z}(z) + B_{2z}(z) = -2a_1 z - 2a_3 z^3 \cdots \quad (5)$$

Since the constant and even-power terms cancel each other out symmetrically, the total field around the central axis becomes an odd function; therefore, near the center, the field is expected to vary linearly with z as a first-order approximation. In Equation 5, a_1 and a_3 are dependent on the magnet dimensions and the distance between the magnets. When the magnet parameters and the gap g between the magnets are properly chosen, the influence of higher-order terms can be neglected in the region between the magnets. In this case, the approximate linear expression for the net magnetic field in the region between the two magnets is given in Equation 6.

$$B_z(z) \cong -2a_1 z \quad (6)$$

As derived in Equations (3)–(5), the symmetrical configuration of the magnets results in the cancellation of even-order harmonic terms in the Taylor series expansion of the magnetic field. Physically, the suppression of these higher-order non-linear terms ensures that the sensor operates within a constant magnetic gradient, which minimizes measurement errors caused by spatial fluctuations. Furthermore, this linearization is crucial for the implementation of sensor systems that incorporate inherently non-linear symmetrical elements, as it simplifies signal processing and enhances measurement accuracy. By displacing the magnet by ±Δ and arranging them such that their magnetization directions face each other, a magnet system is formed as given in Figure 1.ii. Using the magnetic field expression in Equation 6, the magnetic field between the magnets in the system can be obtained as $B_z = Bs_z(z+\Delta) - Bs_z(z-\Delta)$. For this system, the magnetic field at points $O(0,0,-\frac{g}{2} < z < g/2)$ within the gap distance g between the magnets is shown in Figure 3 for a magnet pair with dimensions 3x60x10, where like poles face each other. The gap between the magnets is set as g=3 mm. In Figure 3, the total magnetic field of two magnets with nonlinear magnetic field values can generate an approximately linear magnetic field. However, while the magnetic field of a single magnet at the surface is around 0.33 T, the total magnetic field of the two opposing magnets reaches a maximum of approximately 0.29 T. Although the obtained field is fitted to a linear function ($Bz_{fit} = -254.7536z$), the maximum deviation from the linear curve (Residual) is observed to be around 10 mT. This deviation may cause errors in sensor systems developed using a linear approximation in such magnet configurations.

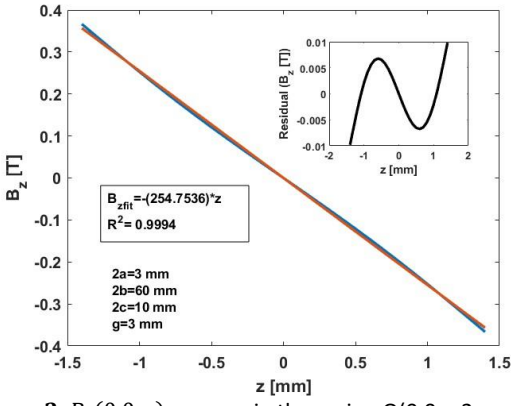

Figure 3. $B_z(0,0,z)$ versus z in the region O(0,0,-g2<z<g/2) for 3x10x60 mm magnet set. Inset: the residual (linearity error).

The linearity of the magnetic field distribution was quantified using the root mean square error (RMSE) and the coefficient of determination (R^2). While R^2

evaluates how well the data fit a linear model (with values closer to 1 indicating higher linearity), RMSE measures the average deviation of the data from the fitted line (with lower values indicating better linearity).

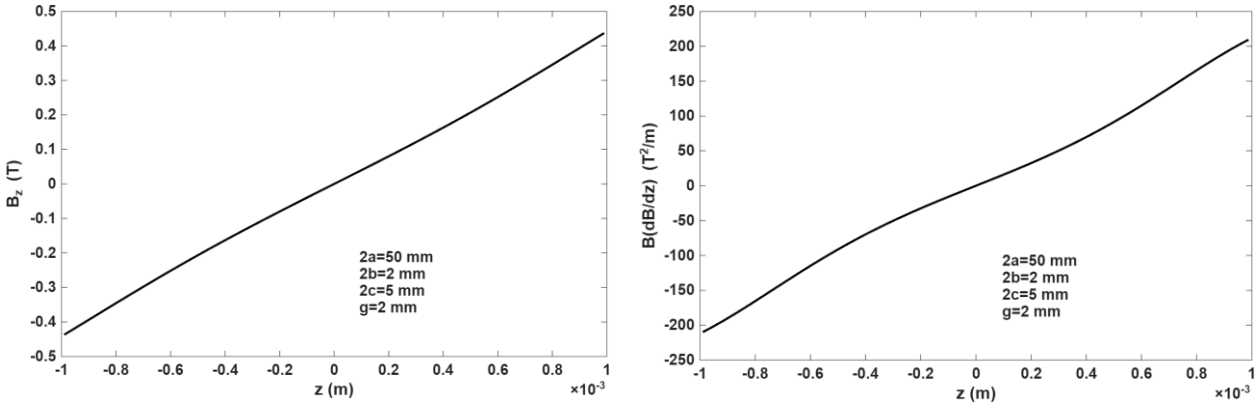

Figure 4. $B_z(0,0,z)$) and $B_z \frac{dB_z}{dz}$ for 50x2x5 mm magnet pair of magnetization M=1050 kA/m.

To validate the numerical calculations, relevant studies from the literature were examined. Several biomedical magnetic levitation (maglev) studies employ a rectangular prism magnet pair with dimensions of 50 × 2 × 5 mm [1,15]. In these studies, simulation results for the magnetic field between the magnets were reported. For comparison, the axial magnetic field $B_z(0,0,z)$of the 50 × 2 × 5 mm magnet pair, along with the corresponding force-related term $B_z \frac{dB_z}{dz}$, were calculated using Equation 2. The calculated results for a gap distance of $g = 2$mm and M=1050 kA/m are shown in Figure 4. An excellent agreement is observed between the numerical results obtained in this study and the simulation results reported by Anil-İnevi *et al.* In particular, the $B_z \frac{dB_z}{dz}$ curve exhibits an identical profile to that shown in Figure 4.

3. Results and Discussions

As shown in Figure 3, it is possible to adjust the separation between the magnets (g) to increase the linearity of magnetic field. This adjustment reduces the influence of higher-order terms (a_3z^3, a_5z^5, ...) in Equation 5, leading the field distribution to approximate the form $B_z(z) \cong -2a_1z$. For this purpose, the air gap was varied from 1 mm to 10 mm in 0.2 mm increments, and the magnetic field distribution along the magnetization direction (z-axis) was calculated using Equations 1 and 2. The computed field was then fitted to a linear function. Afterward, the RMSE [16, 17] and R^2 criteria were evaluated for the fitted function. Figures 5 and 6 present the RMSE and R^2 values for the 3×60×10 mm magnet pair. As seen in Figures 5 and 6, the magnetic field tends to be more linear in regions where the air gap between the magnets is close to zero. However, in these regions, the field strength is relatively low (Table 1), making them less suitable for applications such as magnetic levitation. Therefore, determining the magnet spacing at the local extremum points, where the RMSE value reaches its minimum and the R^2 value reaches its maximum, would be more appropriate, as this ensures both minimal error and the best linear fit. For the magnet pair with dimensions 3×60×10 mm, this optimal range is around 2 mm, corresponding to the region where the magnetic field is closest to linear.

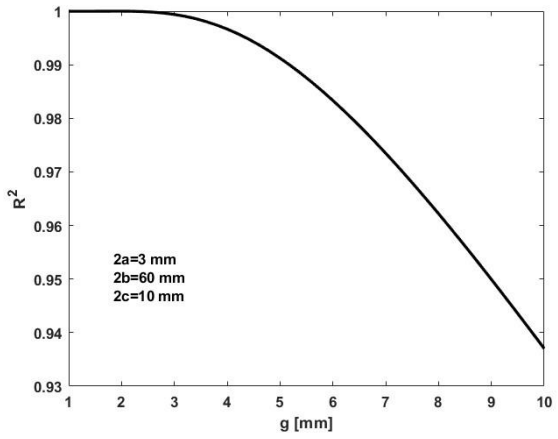

Figure 5. R^2 values for 3x60x10 mm magnet pair.

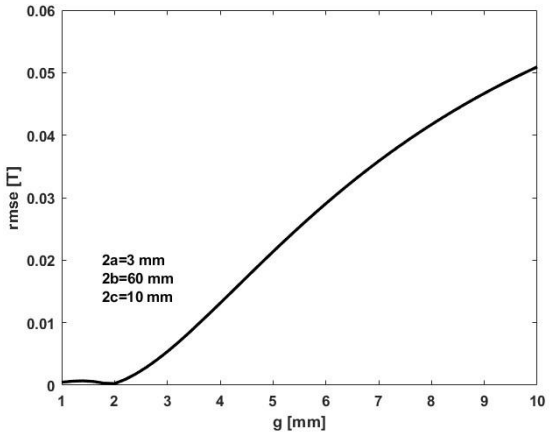

Figure 6. RMSE values for 3x60x10 mm magnet pair.

The g parameter can be selected based on the requirements of the specific physical application. Additionally, the magnetic field strength for the chosen air gap significantly influences the system's efficiency. Table 1 presents the suitability of specific air gaps for linearity and the corresponding maximum magnetic field strength. As seen in Table 1, the optimal air gap value of g=2 mm ensures both the linearity of the magnetic field and an adequate field strength, making it suitable for applications such as magnetic levitation. In addition to the air gap, variations in magnet dimensions also influence the linearity of the field distribution. Figures 7 and 8 present the R^2 and RMSE values for different magnet parameters. As seen in Figures 7 and 8, the optimal point (local minimum) of RMSE graph, varies depending on the geometric parameters. As the gap between the magnet pairs increases, the maximum field strength also increases. Therefore, for any given magnet geometry, it is appropriate to operate at the local maximum of the R^2/g curve (or local minimum of RMSE curve). For 4×40×2 mm magnets, this value is approximately g=3.4 mm, while for 6×20×3 mm magnets, it is around g=6.8 mm.

Table 1. Linearity of certain air gaps and maximum magnetic field strength for 3×60×10 mm magnet pair

Gap between magnets [mm]	RMSE [T/m]	R^2	Maximum magnetic field [T]
1	0.00047	0.99998	0.1705
2	0.00025	0.99999	0.2996
4	0.013	0.9967	0.404
6	0.029	0.98367	0.4428
8	0.041	0.96312	0.4617
10	0.051	0.93869	0.4726

Table 2 presents the optimization results for a series of widely available and easily accessible magnet sets. For the selected magnet dimensions, the gap between the magnets was varied from [0–10] mm, and a linear function was fitted for each interval. The R^2 value was calculated for the fitted function. When selecting the appropriate air gap value for linearity, both the R^2 value and the maximum magnetic field strength along the z axis between the magnets were considered. As observed, the chosen magnet dimensions are critical for both achieving linearity and maximizing the magnetic field strength. Therefore, if the dimensional parameters 2b and 2a are kept constant, the 2c value (the dimension along the magnetization direction) should be as large as possible. Additionally, the rectangular N52-type 50×2×5 mm magnet set was examined in terms of linearity criteria. For N52 magnet pairs with dimensions of 50×2×5 mm, which are frequently used in the literature [18], the air gap providing the closest approach to linearity was determined to be 1.2 mm yielding a maximum magnetic field of $B_z = 0.34$ T. The magnetization for these N52 magnets was set at M=1200 kA/m. Consequently, the disadvantage arising from the relatively low 2c height of the magnet was compensated for by the high magnetization value. Despite having a lower magnetization value (M=930 kA/m), N35 magnet pairs with dimensions of 3×60×10 mm produced similar results to the results similar to those of the N52 50×2×5 mm magnet set. These findings suggest that, with an appropriate selection of magnet dimensions, flexibility can be achieved in the design of magnetic systems for applications such as magnetic levitation and sensor systems.

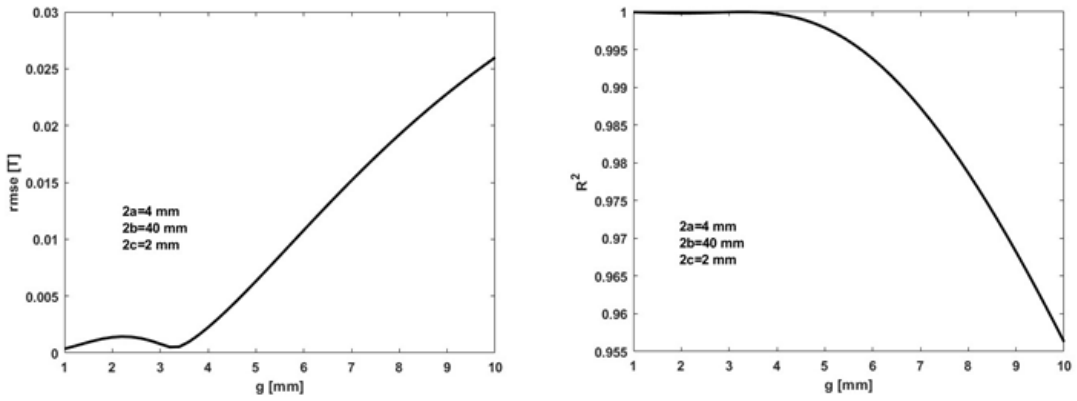

Figure 7. Effect of air gap g variation on RMSE and R^2 values for 4x40x2 mm magnet pairs, illustrating optimal g value.

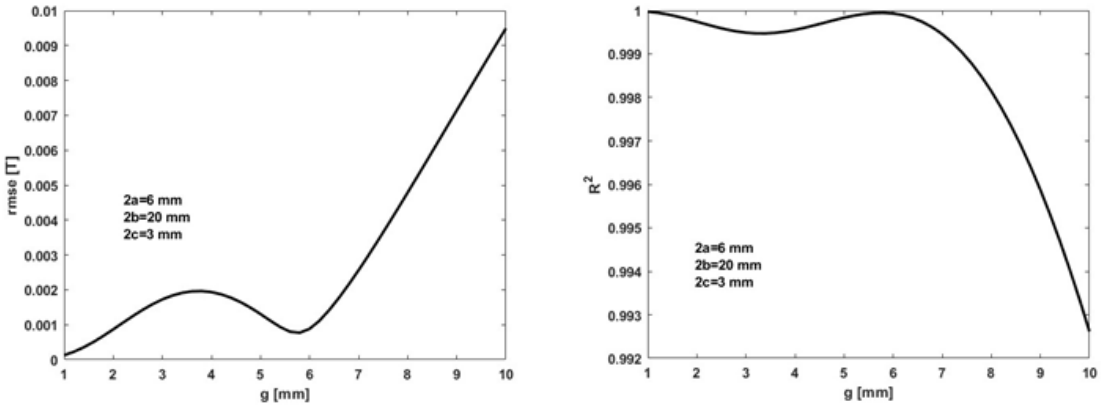

Figure 8. Effect of air gap g variation on RMSE and R^2 values for 6x20x3 mm magnet pairs, illustrating optimal g value.

Table 2. Some of the commercially available magnets and optimum g values for linearity.

Magnet dimensions 2ax2bx2c (mm)	Optimum g (mm)	RMSE (10^{-4} T)	R^2	Maximum magnetic field (T)
2.5x38x14	1.6	1.3	1	0.29
5x40x15	3.2	1.8	0.999	0.31
50x30x10	4	1	0.999	0.04
2x20x10	3.4	8	0.999	0.06
3x60x10	2	2.5	0.999	0.30
50x2x5 (N52)	1.2	3.4	0.999	0.34

The maximum value of $B_z \frac{dB_z}{dz}$ is approximately 200 T^2/m for a 2 mm gap between the magnet pair [15]. The magnets used in this configuration have a magnetization of $M = 1050$ kA/m, which lies within the typical range of 1000–1200 kA/m for N52-grade permanent magnets.

The obtained results are particularly critical for applications requiring high precision and control, such as magnetic levitation systems. Optimizing the magnetic field between magnets enhances the performance of such systems by improving parameters like stability and sensitivity. Furthermore, a detailed analysis of different magnet size and air gap combinations provides valuable insights for the design of displacement sensors, density measurement systems, cell separation, flow focusing, and other biomedical technologies.

The results of this study demonstrate that the magnetic field distribution in the MagLev geometry, as well as magnetic field linearity, are strongly dependent on the magnet geometry and the gap distance between the magnets. Moreover, by appropriately adjusting the magnet dimensions, it is possible to achieve comparable performance using lower-grade magnets instead of higher-grade ones. This observation is consistent with Yu et al. (2023) [18], who established that magnet configuration and geometry are the primary factors governing the tuning of the measurement range and sensitivity of the system. The high linearity (R^2 = 0.9999) observed at a 2 mm gap is also supported by the findings of Zhang et al. (2018) [19], which investigate the linear relationship between levitation height and density. Furthermore, Xie et al. (2019) [20] emphasize that maintaining a precise and accurate magnetic field distribution is essential for achieving high-accuracy density measurements without the need for complex benchmarking procedures. Our results further confirm that optimizing the gap distance as also explored by Rabie et al. (2025) [21] enables a more uniform magnetic force gradient, which is critical for attaining high precision. Consequently, these comparisons suggest that selecting N35 magnets with appropriate dimensions provides a cost-effective and flexible design alternative for MagLev-based biological and material analyses, as discussed in Anil-Inevi et al. (2025) [22].

4. Conclusion

In this study, a linearity analysis based on the gap between magnets was performed for systems with same poles facing each other. While the magnet dimensions are assumed constant, increasing the air gap causes the magnetic field function to deviate from linearity. In this context, for the magnetic system created with a magnet pair of dimensions 3×60×10, an air gap of approximately 1.8–2 mm yields both the maximum magnetic field magnitude and the closest approach to linearity. Additionally, at an air gap of g = 2 mm, the magnetic field fitted to a linear function yielded in R^2 = 0.9999, with a maximum magnetic field value of B_z =0.30 T. The same calculations were performed for different magnet sizes. The variation of the air gap plays a critical role depending on the magnet dimensions. In the R^2 graph calculated for each g value, local maxima indicate the air gap that provides the closest approach to a linear magnetic field function for a given magnet set. For 4×40×2 mm magnets, the R^2 value corresponding to the most linear function is observed around g = 3.4 mm, while for 6×20×3 mm magnets, this value is found at g = 6.8 mm. Additionally, an analysis was conducted on

commercially available magnet pairs, specifying the optimal air gap and the maximum magnetic field value within that range for each magnet pair.

This study makes a significant contribution to literature by advancing the effective design and applicability of magnetic systems. This study also presents significant potential for industrial applications. In particular, optimizing the linearity of the magnetic field can enhance accuracy and reliability in industrial automation systems that require precise displacement measurements and calibration. In such applications, the optimal placement of magnets can ensure long-term operation of systems with minimal maintenance requirements. Consequently, the analytical approaches developed in this study and the obtained results not only contribute to existing applications but also serve as a guide for the design and development of next-generation magnetic systems. Future research could provide optimized solutions for a broader range of applications by conducting a more detailed analysis of different magnet configurations and variations. This has the potential to drive significant advancements in both academic research and commercial applications.

Declaration of Ethical Code

In this study, we undertake that all the rules required to be followed within the scope of the "Higher Education Institutions Scientific Research and Publication Ethics Directive" are complied with, and that none of the actions stated under the heading "Actions Against Scientific Research and Publication Ethics" are not carried out.

References

[1] Delikoyun, K., Yaman, S., Yilmaz, E., Sarigil, O., Anil-Inevi, M., Telli, K., et al. 2021. HologLev: A hybrid magnetic levitation platform integrated with lensless holographic microscopy for density-based cell analysis. ACS Sensors, 6(6), 2191–2201.

[2] Gao, Q.H., Song, P.H., Zou, H.X., Wu, Z.Y., Zhao, L.C., Zhang, W.M. 2025. Three-dimensional manipulation via magnetic levitation. International Journal of Mechanical Sciences, 287, 109949.

[3] Frenea-Robin, M., Marchalot, J. 2022. Basic principles and recent advances in magnetic cell separation. Magnetochemistry, 8(1), 11.

[4] Zhang, C., Zhao, P., Wen, W., Xie, J., Xia, N., Fu, J. 2018. Density-based cell analysis using magnetic levitation. Polymer Testing, 70, 520–525.

[5] Subramaniam, A.B., Yang, D., Yu, H.D., Nemiroski, A., Tricard, S., Ellerbee, A.K., et al. 2014. Noncontact orientation of objects in three-dimensional space using magnetic levitation. Proceedings of the National Academy of Sciences, 111(36), 12980–12985.

[6] Kartal, R.B., Arslan Yildiz, A. 2024. Exploring neuronal differentiation profiles in SH-SY5Y cells through magnetic levitation analysis. ACS Omega, 9(13), 14955–14962.

[7] Xie, J., Zhang, C., Gu, F., Wang, Y., Fu, J., Zhao, P. 2019. An accurate and versatile density measurement device: Magnetic levitation. Sensors and Actuators B: Chemical, 295,

[8] Netzer, Y. 1981. A very linear noncontact displacement measurement with a Hall-element magnetic sensor. Proceedings of the IEEE, 69(4), 491–492.

[9] Roumenin, C.S., Lozanova, S.V. 2007. Linear displacement sensor using a new CMOS double-Hall device. Sensors and Actuators A: Physical, 138(1), 37–43.

[10] He, Q., Fan, S., Chen, N., Tan, R., Chen, F., Fan, D. 2021. Analysis of inductive displacement sensors with large range and nanoscale resolution. Applied Sciences, 11(21), 10134.

[11] Hancox, C.I., Doret, S.C., Hummon, M.T., Luo, L., Doyle, J.M. 2004. Magnetic trapping of rare-earth atoms at millikelvin temperatures. Nature, 431(7006), 281–284.

[12] Anil-Inevi, M., Yaman, S., Yildiz, A.A., Mese, G., Yalcin-Ozuysal, O., Tekin, H.C., Ozcivici, E. 2018. Biofabrication of in situ self-assembled 3D cell cultures in a weightlessness environment generated using magnetic levitation. Scientific Reports, 8(1), 7239.

[13] Camacho, J.M., Sosa, V. 2013. Alternative method to calculate the magnetic field of permanent magnets with azimuthal symmetry. Revista Mexicana de Física E, 59(1), 8–17.

[14] Edwards, C., Palmer, S.B. 1986. The magnetic leakage field of surface-breaking cracks. Journal of Physics D: Applied Physics, 19(4), 657.

[15] Anil-Inevi, M., Sarigil, O., Unal, Y.C., Tekin, H.C., Mese, G., Ozcivici, E. 2025. Magnetic levitation-based determination of single-nuclei density. Biomaterials Advances, 214581.

[16] Shah, A.S., Karabulut, M.A. 2022. Reliability estimation for drone communications by using an MLP-based model. International Advanced Researches and Engineering Journal, 6(3), 204–210.

[17] Ergül, B., Yıldız, Z. 2023. Comparison of classical and robust factor analyses methods. Süleyman Demirel Üniversitesi Fen Bilimleri Enstitüsü Dergisi, 27(3), 401–410.

[18] Durmus, N.G., Tekin, H.C., Guven, S., Sridhar, K., Arslan Yildiz, A., Calibasi, G., et al. 2015. Magnetic levitation of single cells. Proceedings of the

National Academy of Sciences, 112(28), E3661–E3668.

[19] Yu, J., Li, D., Zhu, C., Ouyang, Q., Miao, C., Yu, H. 2023. A magnetic levitation system for range/sensitivity-tunable measurement of density. Sensors, 23(8), 3955.

[20] Zhang, C., Zhao, P., Wen, W., Xie, J., Xia, N., Fu, J. 2018. Density measurement via magnetic levitation: linear relationship investigation. Polymer Testing, 70, 520–525.

[21] Xie, J., Zhang, C., Gu, F., Wang, Y., Fu, J., Zhao, P. 2019. An accurate and versatile density measurement device: Magnetic levitation. Sensors and Actuators B: Chemical, 295, 204–214.

[22] Rabie, M., Ibrahim, S.S., Eltawil, A.A., Sayed, B.M. 2025. Investigation of the accurate hybrid automatic magnetic levitation system for measuring the high density of material. Measurement, 118866.

[23] Anil-Inevi, M., Sarigil, O., Unal, Y.C., Tekin, H.C., Mese, G., Ozcivici, E. 2025. Magnetic levitation-based determination of single-nuclei density. Biomaterials Advances, 214581.